



HAL
open science

Cluster Observations of Energetic Electron Acceleration Within Earthward Reconnection Jet and Associated Magnetic Flux Rope

A. Vaivads, Yu. Khotyaintsev, A. Retinò, H. Fu, E. Kronberg, P. Daly

► **To cite this version:**

A. Vaivads, Yu. Khotyaintsev, A. Retinò, H. Fu, E. Kronberg, et al.. Cluster Observations of Energetic Electron Acceleration Within Earthward Reconnection Jet and Associated Magnetic Flux Rope. Journal of Geophysical Research Space Physics, 2021, 126 (8), 10.1029/2021JA029545 . hal-03390211

HAL Id: hal-03390211

<https://hal.science/hal-03390211>

Submitted on 22 Nov 2021

HAL is a multi-disciplinary open access archive for the deposit and dissemination of scientific research documents, whether they are published or not. The documents may come from teaching and research institutions in France or abroad, or from public or private research centers.

L'archive ouverte pluridisciplinaire **HAL**, est destinée au dépôt et à la diffusion de documents scientifiques de niveau recherche, publiés ou non, émanant des établissements d'enseignement et de recherche français ou étrangers, des laboratoires publics ou privés.

1 **Cluster observations of energetic electron acceleration**
 2 **within earthward reconnection jet and associated**
 3 **magnetic flux rope**

4 **A. Vaivads¹, Yu. V. Khotyaintsev², A. Retinò³, H. S. Fu⁴, E. A. Kronberg⁵, P.**
 5 **W. Daly⁶**

6 ¹Space and Plasma Physics, School of Electrical Engineering and Computer Science, KTH Royal Institute
 7 of Technology, Sweden

8 ²Swedish Institute of Space Physics, Uppsala, Sweden

9 ³Laboratoire de Physique des Plasmas LPP, Centre National de la Recherche Scientifique CNRS, France

10 ⁴School of Space and Environment, Beihang University, Beijing, China

11 ⁵Department of Earth and Environmental Sciences, University of Munich, Munich, Germany

12 ⁶Max Planck Institute for Solar System Research, Göttingen, Germany

13 **Key Points:**

- 14 • Detailed study of energetic electron acceleration in the braking region of earth-
 15 ward propagating reconnection jet
- 16 • Large electron acceleration in the magnetic flux pile-up region and in the turbu-
 17 lent region containing a magnetic flux rope in front of the jet
- 18 • The largest energetic electron fluxes are inside the flux rope, probably due to Fermi
 19 acceleration process

Corresponding author: A.Vaivads, vaivads@kth.se

20 **Abstract**

21 We study acceleration of energetic electrons in an earthward plasma jet due to magnetic
 22 reconnection in the Earth magnetotail for one case observed by Cluster. The case has
 23 been selected due to the presence of high fluxes of energetic electrons, Cluster being in
 24 the burst mode and Cluster separation being around 1000 km that is optimal for stud-
 25 ies of ion scale physics. We show that two characteristic acceleration mechanisms are op-
 26 erating during this event. First, significant acceleration is achieved inside the magnetic
 27 flux pile-up of the jet, the acceleration mechanism being consistent with betatron accel-
 28 eration. Second, strong energetic electron acceleration occurs in magnetic flux rope like
 29 structure forming in front of the magnetic flux pile-up region. Energetic electrons inside
 30 the magnetic flux rope are accelerated predominantly in the field-aligned direction and
 31 the acceleration can be due to Fermi acceleration in a contracting flux rope.

32 **1 Introduction**

33 High-speed jets created by the magnetic reconnection process are one of the ma-
 34 jor source regions of suprathermal/energetic electrons in astrophysical plasmas. The near-
 35 Earth space, particularly magnetotail, is an ideal place to make experimental observa-
 36 tions of the regions where those electrons are accelerated (Birn et al., 2012; Sitnov et al.,
 37 2019). Statistical studies have shown that highest electron fluxes are occurring closer to
 38 the Earth where the magnetic field gets more dipolar (Åsnes et al., 2008; Luo et al., 2011).
 39 According to observations and numerical simulations one of important driver of electron
 40 energization is the reconnection process that allows electron acceleration both close to
 41 the reconnection site as well as in the regions of outflow jets (Birn et al., 2012; Hoshino
 42 et al., 2001; Imada et al., 2007).

43 One region of particular importance for the electron acceleration is the region where
 44 earthward jets are braking against the dipolar field lines of near-Earth magnetosphere
 45 (Khotyaintsev et al., 2011; Malykhin, Grigorenko, Kronberg, & Daly, 2018). Detailed
 46 studies of selected events show that magnetic pile-up regions, also called dipolarization
 47 fronts, forming in front of the reconnection jets can contain high fluxes of energetic elec-
 48 trons accelerated due to both betatron and Fermi acceleration mechanisms (Fu et al., 2011;
 49 Birn et al., 2012; Fu et al., 2013). It has also been shown on an event-case basis that the
 50 region where reconnection jets are braking against the dipolar field are associated with
 51 high fluxes of energetic electrons (Vaivads et al., 2011; Malykhin, Grigorenko, Kronberg,
 52 Koleva, et al., 2018). However, there are still open questions regarding which are the most
 53 efficient acceleration processes and what is the relative contribution of the various pro-
 54 cesses.

55 Different studies have pointed out that magnetic islands or flux ropes can contribute
 56 to the acceleration of electrons. Particularly, a recent study using ARTEMIS data from
 57 tailward flows and comparisons with 2D PIC numerical simulations suggested that en-
 58 ergetic electrons are correlated to the center of the magnetic islands (Lu et al., 2020). Mag-
 59 netic flux ropes on much smaller scale associated with energetic electrons has been re-
 60 ported earlier also as seen by Cluster spacecraft (Retinò et al., 2008; Huang et al., 2012;
 61 Chen et al., 2008). Detailed MMS observations within a magnetic flux rope produced
 62 by reconnection showed a difference in the acceleration on both sides of the island and
 63 identified the betatron acceleration mechanism as the dominant player (Zhong et al., 2020).
 64 Statistical studies of magnetic flux ropes have shown that only about one fourth of them
 65 show increased fluxes of energetic electrons (Borg et al., 2012). Numerical simulations have
 66 shown energetic electron production in kinetic scale flux ropes (Oka, Fujimoto, et al., 2010;
 67 Oka, Phan, et al., 2010). The important role of ion-scales magnetic flux ropes for gen-
 68 eration of energetic electrons has been shown also in large-scale simulations (Zhou et al.,
 69 2018).

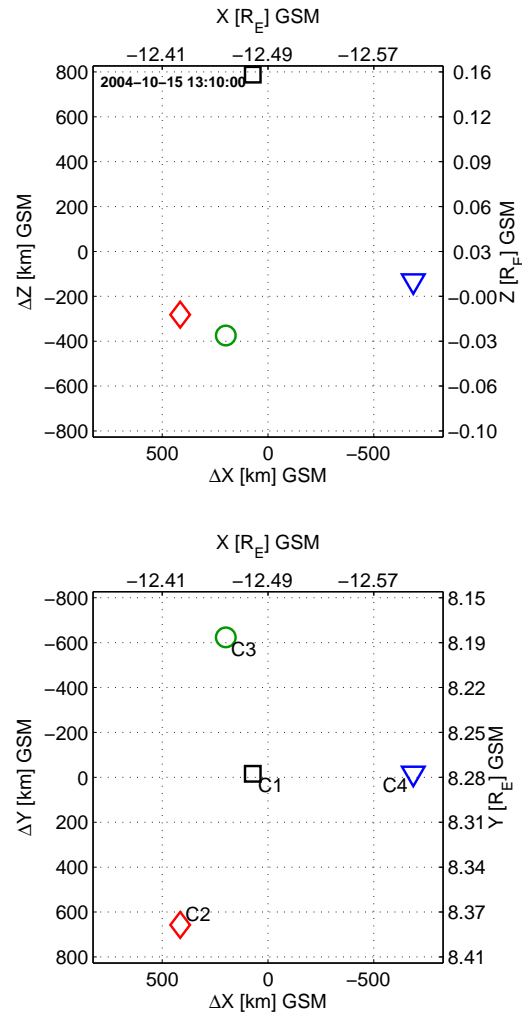


Figure 1. Cluster location and configuration in GSM reference frame.

70 The reconnection jet fronts can be one of the places of the magnetic island forma-
 71 tion. Recent high resolution numerical simulations have shown the process of island forma-
 72 tion in front of reconnection jets, however they could not study the energetic electron
 73 properties(Lapenta et al., 2015). The experimental observations of such island forma-
 74 tion are scarce. In this paper we present a detailed study of a single event showing high
 75 fluxes of energetic electrons generated inside kinetic-scale magnetic flux rope in front of
 76 the reconnection jet and associated magnetic pile-up region.

77 **2 Observations**

78 We have selected for deeper study one event of high suprathermal/energetic electron
 79 fluxes associated with the reconnection jet in the Earth’s magnetotail based on sev-
 80 eral criteria: 1) Cluster is in the magnetotail, 2) the presence of strong energetic elec-
 81 tron acceleration, 3) reconnection jet associated with a magnetic flux pile-up region, 4)
 82 Cluster separation is comparable to the ion scales allowing us to study microphysics of
 83 energetic electron acceleration, 5) Cluster is running in Burst Mode (high telemetry mode),
 84 providing the highest resolution data from both field and particle instruments. Based

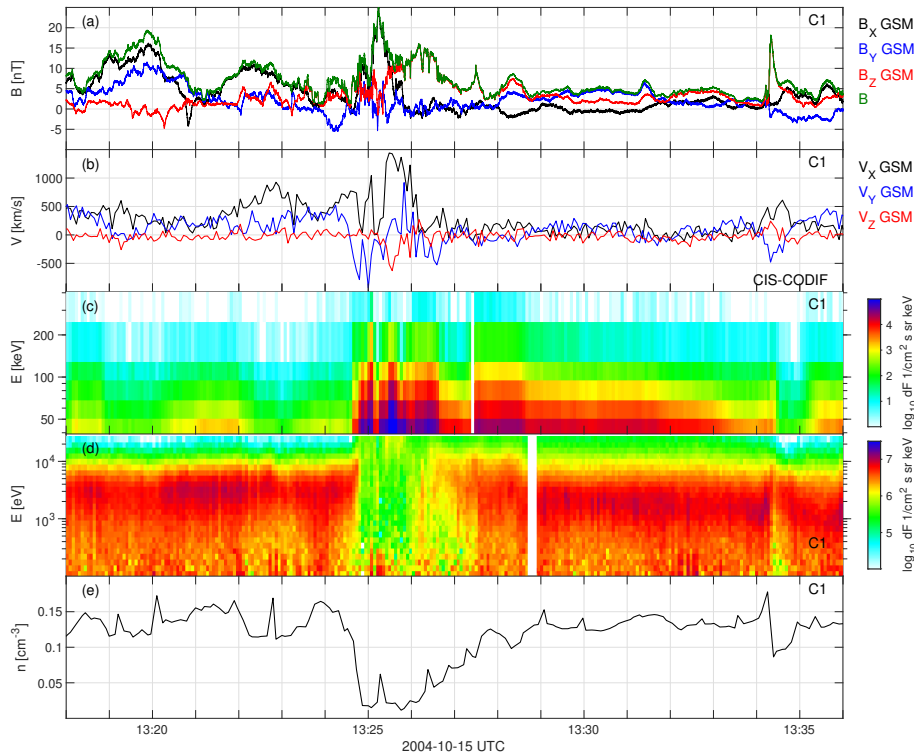


Figure 2. Event overview as seen by C1. (a) Magnetic field in GSM coordinates, (b) ion velocity as measured by the CIS-CODIF instrument, (c) energetic electron differential number flux, measured by RAPID, (d) electron differential number flux, measured by PEACE, (e) electron density measured by PEACE.

85 on these criteria we could identify several events. For the detailed study presented in this
 86 paper we select the event around 2004-10-15 13:26 UT.

87 During the selected event Cluster is located close to the neutral sheet at $[-12.5, 8.3,$
 88 $0] R_E$ GSM, see Figure 1. The Cluster separation is ~ 1000 km which is comparable to
 89 a characteristic local ion scale, which is the gyroradius of 10 keV proton in 10 nT field
 90 $\rho_i \sim 1400$ km. Of particular importance for the paper will be that C4 is located most
 91 tailward and C1 is located most northward.

92 We use measurements of magnetic field (FGM instrument), electric field (EFW),
 93 ions (CIS) and electrons (PEACE, RAPID) (Escoubet et al., 1997). During the event
 94 Cluster was in the Burst Mode (high-telemetry mode) allowing detailed and high-time
 95 resolution measurements of particles and fields. We identify the four Cluster spacecraft
 96 as C1, C2, C3 and C4.

97 Figure 2 shows the large-scale context of the event as seen by Cluster spacecraft
 98 C1. During most of the event $|B_X|$ is close to zero or is small in comparison to its ex-
 99 pected lobe field value of ~ 20 nT, see Figure 2a. Thus C1 is located inside the plasma
 100 sheet close to the neutral sheet. Similar argument applies to the other Cluster spacecraft
 101 (not shown). The plasma sheet can be also identified by the presence of several keV hot
 102 thermal electrons, see Figure 2d. Plasma ions show earthward flows throughout the in-
 103 terval, $V_X > 0$ in Figure 2b, being the highest in the beginning of the interval with the
 104 peak reaching 1500 km/s at 13:25:30 UT. Around the peak of V_X we observe an increase

105 in B_Z , and the region of increased B_z (flux pile-up region) continues for a few minutes
 106 after the peak in velocity. Also, around the V_X peak we observe a significant density de-
 107 crease, Figure 2e. All these signatures are characteristic for earthward jets produced by
 108 the reconnection tailward of the spacecraft. Figure 2c shows the energetic electron spec-
 109 trogram, by energetic we mean the electron energies are tens of times larger than the ther-
 110 mal energy of electrons. Very strong increase in energetic electron fluxes is seen in as-
 111 sociation with the ion jet and magnetic flux pile-up region. The magnetic flux pile-up
 112 region and its associated energetic electron generation is the focus of this paper.

113 There is another smaller magnetic flux pile-up region during the second part of in-
 114 terval in Figure 2. There are ion flows with a localize peak of about 500 km/s around
 115 13:34:30 UT and distinct magnetic flux pile-up associated to this peak. However, there
 116 are no associated peak in energetic electron flux. It is interesting to note that the sec-
 117 ond pile-up region was included in a large statistical study (Fu et al., 2012) analyzing
 118 energetic electron acceleration at the dipolarization fronts, while the first one is not. The
 119 reason for this is that the second pile-up region has a very distinct and sharp front which
 120 was used as a condition for event selection in previous studies (Fu et al., 2012). The first
 121 pile-up region does not have such a front, but it is associated with strong energetic elec-
 122 tron acceleration. This indicates that many pile-up regions with strong energetic elec-
 123 tron generation may be missed by earlier studies of dipolarization fronts due to their com-
 124 plex front structure. We return in the discussion part to the possible reasons why sec-
 125 ond pile-up region does not show any signs of energetic electron generation.

126 Figure 3 shows detailed observations of the first magnetic flux pile-up region as seen
 127 by all four Cluster spacecraft during a 3 min interval. Figure 3a shows the magnitude
 128 of magnetic field. The low values of $|B|$ indicate that spacecraft are inside the plasma
 129 sheet close to the neutral sheet. Only during the short interval around 13:25:15 UT C1
 130 is observing B larger than 20 nT indicating that C1 enters into the lobe during that time
 131 period. Figure 3b shows that all spacecraft observed magnetic flux pile-up, seen as in-
 132 crease in the B_Z . All spacecraft observe the entering into the pile-up region almost si-
 133 multaneously consistent with pile-up region passing spacecraft with high speed. How-
 134 ever, the exiting of the pile-up region takes much longer time and thus the boundary is
 135 moving slowly, consistent with ion velocity in Figure 2. We can also see that C4 is the
 136 first that sees the B_Z decrease after the passage of the pile-up region, This is consistent
 137 with C4 being the most tailward spacecraft, see Figure 1. Figure 3c shows the sunward
 138 velocities (X-component in ISR2 reference frame) estimated from $\mathbf{E} \times \mathbf{B}$ -drift and mea-
 139 sured by the ion spectrometer. The ISR2 reference frame is individual to each of the satel-
 140 lites, it is close to GSE but has X and Y components in the satellite spin plane. In gen-
 141 eral $\mathbf{E} \times \mathbf{B}$ velocities are higher than ion drift velocities, consistent with ion instrument
 142 not being able to observe all thermal ions due to their high thermal energy which ex-
 143 ceeds the maximum energy which can be measured by the CODIF instrument. Figure
 144 3d shows the velocity component in the dawn-dusk direction (ISR2 Y). Large flow in the
 145 dawn direction can be seen before the magnetic pile-up. During the peak sunward ve-
 146 locity, there is no significant ISR2 Y-component of velocity. Figure 3e shows the ener-
 147 getic electrons flux observed by C4. There is a general increase of energetic electron flux
 148 associated with the sunward flow seen both before and during the magnetic flux pile-up
 149 region. However, the peak fluxes are very localized and there can be large change be-
 150 tween the measurements performed during the consecutive spacecraft spins (satellite spin
 151 is 4 s). The last two panels Figure 3f,g show current and $\mathbf{j} \times \mathbf{B}$ force estimates based on
 152 the multi-spacecraft curlometer technique. A significant positive j_Y can be seen in Fig-
 153 ure 3f during the first half of the interval, while the current gets weak during the sec-
 154 ond half where the plasma velocity is small and B_Z dominates. Figure 3g shows the $\mathbf{j} \times \mathbf{B}$
 155 force acting on plasma. There is a significant positive $(\mathbf{j} \times \mathbf{B})_X$ during the first half of
 156 the interval corresponding to the earthward jet. In the center of interval there is a sig-
 157 nificant negative $(\mathbf{j} \times \mathbf{B})_Z$ as the spacecraft constellation is slightly above the center of

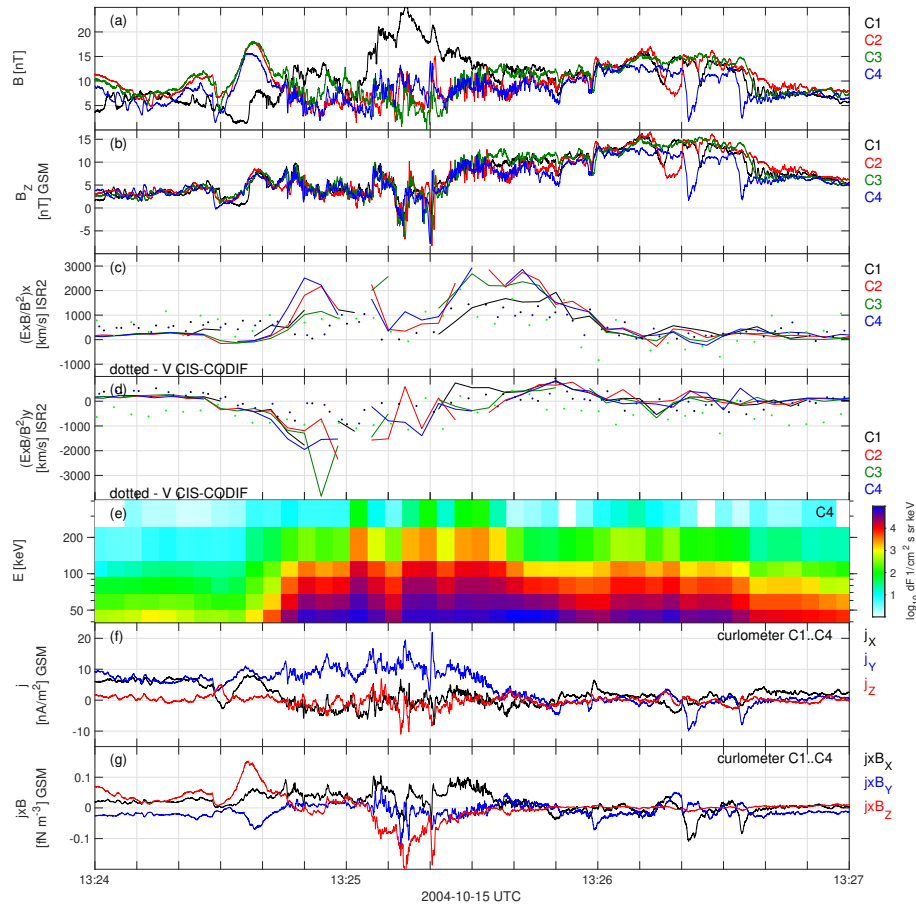


Figure 3. Multi-spacecraft overview. (a) The magnitude of magnetic field, (b) B_z GSM, (c) V_x ISR2 from CIS-CODIF measurements and from $\mathbf{E} \times \mathbf{B}$ -velocity estimates using electric field measurement, (d) same but for Y ISR2 component, (e) energetic electron differential flux as seen by C4, (f) current estimate based on the curlometer method, (g) $\mathbf{j} \times \mathbf{B}$ -force based on the curlometer method.

158 the current sheet. The negative $(\mathbf{j} \times \mathbf{B})_y$ in the beginning of the interval is consistent
 159 with strong plasma flows in the $-Y$ direction.

160 Figure 4 shows detailed observations of the pile-up region and energetic electrons
 161 as seen by all Cluster spacecraft. Figure 4a shows magnetic field B_z GSM. The pile-up
 162 region is reached around 13:25:30 UT when B_z reaches steady values of about 10 nT. Next
 163 four panels, Figure 4b-e, show the pitch angle distribution of energetic electrons at ~ 60 keV
 164 energy. To understand the details of the energization process, we are plotting the sub-
 165 spin resolution data. The electron instrument provides the full 3D distribution during
 166 a full spin. However, assuming that electrons are gyrotropic, we can use instantaneous
 167 2D measurements during the spin (subspin resolution) to cover a limited range of pitch-
 168 angles. This range will vary during the spin due to varying orientation of \mathbf{B} relative to
 169 the 2D plane of the measurement and this variation can be clearly seen in the plot. The
 170 grey areas show regions that have not been accessible to the measurement. C1 observes
 171 the lowest fluxes because C1 is the furthest away from the center of the current sheet
 172 as can be seen from C1 having largest B values in Figure 3a. As adiabatic acceleration
 173 mechanisms involve changes in magnetic field magnitude, we overplot the magnitude of

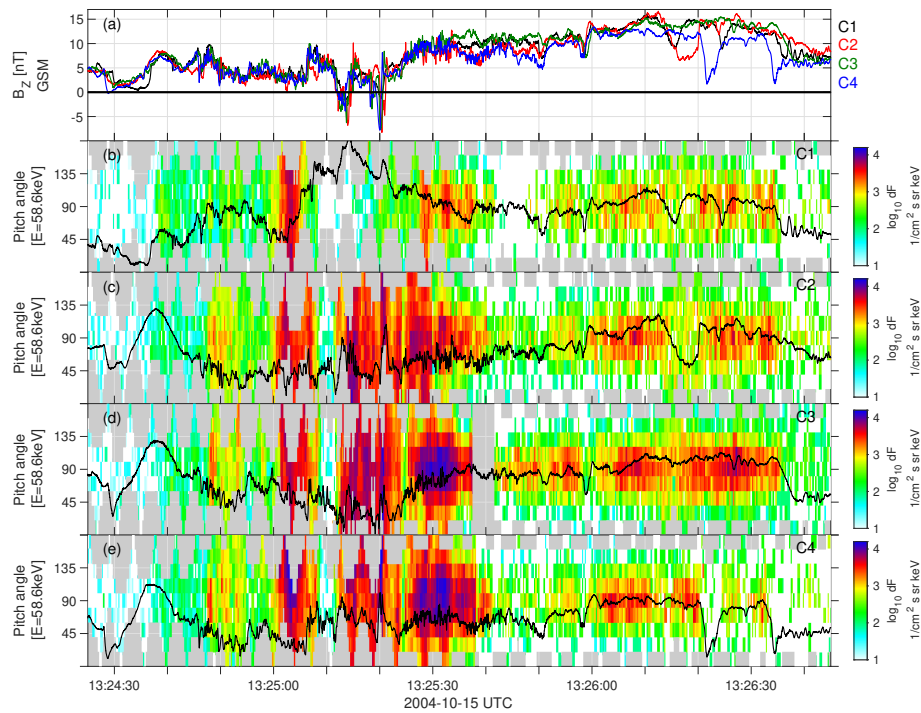


Figure 4. Magnetic pile-up region and energetic electron anisotropies. (a) B_z in GSM from all Cluster spacecraft, (b-e) pitch angle spectrogram of energetic electrons corresponding to the RAPID channel of 60 keV at subspin resolution, the areas marked in gray correspond to pitch angles not accessible for measurement during that moment of the spin and the white areas correspond to low or zero fluxes.

174 B (solid line) on top of electron spectrograms. Several important observations can be
 175 noted. 1) During the maximum of magnetic pile-up, around 13:26:00-13:26:40, there is
 176 a clear increase in energetic electron fluxes and the highest fluxes are close to 90 degree
 177 pitch angles. However, this is not the region of the highest fluxes. The highest fluxes are
 178 observed in the interval 13:25:00-13:25:40 UT which corresponds to the region before the
 179 pile-up and the beginning of the pile-up region. During this time period the highest sun-
 180 ward velocities are observed, see Figure 3c. Inside the beginning of the pile-up region elec-
 181 trons are dominated by fluxes close to 90 degree pitch angles. Before the pile-up region
 182 there is no clear pitch-angle dependence and the magnetic field is highly variable. We
 183 focus on this region in even more detail.

184 To better identify the location of the most energetic electrons with respect to the
 185 magnetic structure, Figure 5 shows an additional zoom in. Figure 5a shows B_z GSM and
 186 Figure 5b-d show C2-C4 energetic electron spectrograms, those satellites are closest to
 187 the current sheet and observe the largest fluxes. The color-scale of the electron spectro-
 188 grams has been changed to better identify the most energetic electrons. The largest fluxes
 189 are seen by C3 and C4. Inside the pile-up region there is a wide region of high flux with
 190 the peak at 90 degree pitch angle. However, also at subspin resolution the highest elec-
 191 tron fluxes are highly varying. There is another region, just after 13:25:20 UT where very
 192 high electron fluxes are briefly (for just a few energy sweeps) observed. In this region the
 193 instrument observes the highest instantaneous electron fluxes during the whole event.
 194 In the discussion we argue that this region is consistent with being a magnetic flux rope.
 195 There are several important observations related to these electrons. 1) Magnetic field

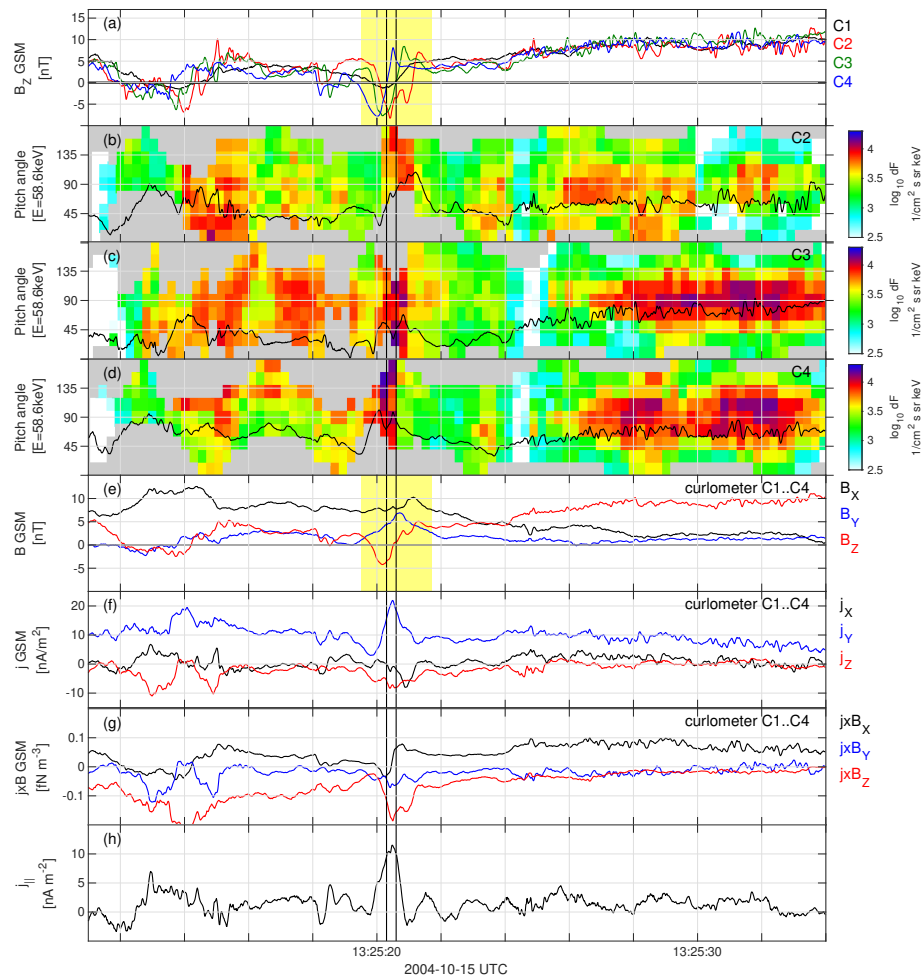


Figure 5. Zoom in around the front of magnetic flux pile-up region. (a) B_Z in GSM from all Cluster spacecraft, the region of negative/positive variation is marked yellow. (b-d) C2-C4 pitch angle spectrogram of energetic electrons corresponding to the RAPID channel of 60 keV at subspin resolution, the areas marked in gray correspond to pitch angles not accessible for measurement during that moment of the spin. (e-f) Observations based on all four spacecraft measurements: (e) average magnetic field, (f) current estimate based on curlometer method, (g) $\mathbf{j} \times \mathbf{B}$ force based on curlometer method, (h) current parallel to the ambient magnetic field.

196 shows a negative-positive bipolar B_Z variation near the region of the highest fluxes, the
 197 region is marked yellow in Figure 5a. 2) The peak fluxes on C3 and C4 coincide with the
 198 center of bipolar B_Z variation. The center of the bipolar structures where B_Z crosses
 199 zero (going from negative to positive values) are marked by solid lines for C3 and C4 re-
 200 spectively. 3) The magnitude of magnetic field shows a dip at the location of the high-
 201 est fluxes at C3 and C4. 4) The highest fluxes of electrons are not necessary centred around
 202 90 degree pitch angle. There even seems to be a tendency for electrons to be more field-
 203 aligned than perpendicular. 5) C2 sees lower electrons fluxes, there is no dip in magnetic
 204 field magnitude and also the bipolar structure is less clear. We will discuss later that these
 205 observations are consistent with the presence of a magnetic flux rope.

206 To better characterize this magnetic structure in Figure 5e-h we plot various quan-
 207 tities computed using 4-point measurements by Cluster. Figure 5e shows the average mag-
 208 netic field. It can be seen that during the time of the bipolar B_Z variation there is also
 209 a strong B_Y component. Such a B_Y component is consistent with core field of magnetic
 210 flux rope as we will show in the discussion part. Figure 5f shows the current, the peak
 211 in the current is coinciding with the region of highest energetic electron fluxes. Figure 5g
 212 shows $\mathbf{j} \times \mathbf{B}$ force. During the whole interval $(\mathbf{j} \times \mathbf{B})_X$ is mainly positive, and around
 213 the highest fluxes one can see a bipolar negative/positive signature in $(\mathbf{j} \times \mathbf{B})_X$. Finally,
 214 Figure 5h shows the current parallel to the average magnetic field j_{\parallel} , and we can see a
 215 strong peak in j_{\parallel} coinciding with the location of high energetic electron fluxes.

216 3 Discussion

217 Based on the observations presented above we can make the overall interpretation
 218 of the event. During the time interval 13:25-13:26 we see high-speed earthward jet that
 219 reaches above 1000 km/s in ion data and more than 2000 km/s in $\mathbf{E} \times \mathbf{B}$ -velocity. This
 220 is consistent with an observation of an earthward reconnection jet. The energies of ther-
 221 mal ions reach above the energy range of the CODIF instrument used to estimate the
 222 velocity moment and therefore the ion velocity shows values lower than the $\mathbf{E} \times \mathbf{B}$ ve-
 223 locity. During about 2 min following the peak of the jet velocity we observe a region where
 224 B_Z is dominating, with the B_Z values of the order of 10 nT. We interpret this as the mag-
 225 netic flux pile-up region driven by the jet. However, during the last part of the B_Z -dominated
 226 region V_X decreases to small values and even reverses the sign. This suggests that space-
 227 craft are on the dipolar field lines close to the jet braking region. Thus the spacecraft
 228 are located in the right region to observe the incoming magnetic pile-up region driven
 229 by the reconnection jet, how it brakes due to the near Earth dipolar-like field and how
 230 the jet driven magnetic pile-up becomes part of the near Earth dipolar field. Additional
 231 support for this hypothesis comes from the j_Y observations, see Figure 3. In the begin-
 232 ning of the interval j_Y is strong and positive both before and in the beginning of the mag-
 233 netic flux pile-up region. This is consistent with spacecraft located in the thin current
 234 sheet in the beginning of the interval followed by reconnection jet driven magnetic flux
 235 pile-up. As the jet brakes and its velocity decreases to zero also j_Y value goes to zero
 236 consistent with spacecraft being on dipolar field lines. Finally, on the exit boundary of
 237 dipolar like field region j_Y is negative as expected when being on the outer region of dipol-
 238 ar field lines. Thus, we are observing the whole chain consisting of the onset of fast re-
 239 connection jet, followed by jet braking and spacecraft location close to the dipolar field
 240 lines where the jet brakes.

241 During the interval of jet we observe significantly increased energetic (40-400keV)
 242 electron fluxes. The Cluster separation of ~ 1000 km comparable to characteristic ions
 243 scales allows for detailed exploration of energetic electron acceleration. We observe that
 244 there are several mechanisms in play providing the acceleration. In the pile-up region
 245 the dominant acceleration is occurring at close to 90 degree pitch angles, with the high-
 246 est fluxes observed at 13:25:30 UT simultaneous with the detection of the highest jet ve-
 247 locities. Thus, this region is most probably a magnetic flux pile-up region driven by the
 248 reconnection jet and what we observe is the betatron acceleration as has been reported
 249 in earlier studies (Khotyaintsev et al., 2011; Fu et al., 2011). However, high fluxes of en-
 250 ergetic electrons are also observed in the turbulent region in front of the pile-up region,
 251 as can be clearly seen in Figure 4 and Figure 5. Closer inspection of data in Figure 5 shows
 252 that this turbulent region contains the highest electron fluxes during the whole event (ob-
 253 served during a short time interval around 13:25:20 UT).

254 Multi-spacecraft observations allow to clearly identify the structure of the region
 255 with the highest electron fluxes at 13:25:20 UT. The magnetic field observations are con-
 256 sistent with it being a flux-rope-like structure: a negative-positive B_Z variation for earth-
 257 ward moving structure, converging $\mathbf{j} \times \mathbf{B}$ force, strong parallel current in the center of

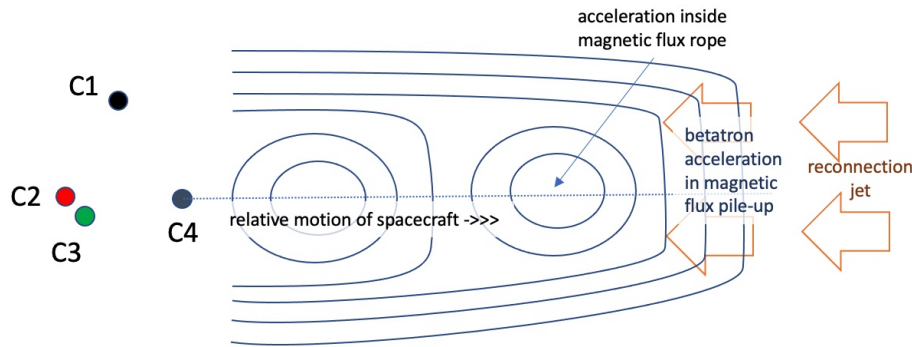


Figure 6. Simplified sketch showing the location of Cluster spacecraft with respect to the current sheet and how they cross the magnetic island and magnetic flux pile-up region.

258 the structure and a significant core field B_Y . The characteristic cross-section of the flux
 259 rope is of the order of the spacecraft separation (ion scales). This is observed both in
 260 the X-direction and Z-direction. In the X-direction the two spacecraft separated in X-
 261 direction, C2 and C4, simultaneously observe peak values of B_Z of opposite sign con-
 262 sistent with C2-C4 separation being comparable to the flux rope size. In the Z-direction,
 263 C1 is separated by ~ 1000 km from the other 3 spacecraft, and while C1 sees lobe field
 264 values the other 3 spacecraft are still near the center of the current sheet; this is also con-
 265 sistent with the flux-rope scale being comparable to the spacecraft separation. Figure 6
 266 summarizes in a simplified sketch the characteristic separation of spacecraft in compar-
 267 ison to the thickness of the current sheet and the size of magnetic island and illustrates
 268 how the spacecraft cross the flux rope.

269 There have been studies showing presence of high fluxes of energetic electrons in
 270 kinetic-scale magnetic islands in the thin current sheet close to the reconnection onset (Retinò
 271 et al., 2008; Huang et al., 2012). Both studies show that the highest electron fluxes were
 272 detected in the center of magnetic island, while the island was embedded into a thin re-
 273 connecting current sheet. When it was possible to measure pitch angle distribution, it
 274 was concluded that main acceleration is of energetic electrons at perpendicular direction
 275 to the magnetic field. The study by Retinò et al. (2008) also analyzed the pitch-angle
 276 distribution and found the highest fluxes for electrons close to 90 degree pitch angles sug-
 277 gesting that they can be energized by the betatron mechanism. Similarly, there is a case
 278 study using the MMS observations of energetic electrons inside an ion-scale magnetic is-
 279 land with perpendicular acceleration of electrons (Zhong et al., 2020). Here, we show that
 280 magnetic islands can also form in front of the magnetic pile-up region driven by the re-
 281 connection jet. In addition, we show that other acceleration mechanisms than betatron
 282 acceleration can be at play in the center of the magnetic island. This is related to the
 283 fact that we observe the dominant acceleration in field-aligned direction, and not in the
 284 perpendicular direction as expected for the betatron mechanism.

285 There can be several possible electron acceleration mechanisms inside the flux rope.
 286 One is the direct acceleration by the parallel electric field (Pritchett, 2006). The pres-
 287 ence of the strong parallel current in the center of the flux rope suggest that there should
 288 be also strong parallel fields forming leading to acceleration of electrons in the anti-parallel
 289 direction. The presence of parallel fields inside the flux ropes is indirectly supported by
 290 observations of electron holes inside the ropes (Khotyaintsev et al., 2010). There is some
 291 indication in data, see Figure 5, that C4 which looks in the anti-parallel direction detects
 292 the highest fluxes, however, there are too few data points to make a solid conclusion. It
 293 is also seen, that C3 that is looking predominantly in the parallel direction also sees in-

294 creased electron fluxes. Thus there should be additional acceleration mechanisms in play,
 295 such as wave-particle interaction or Fermi acceleration in contracting flux rope (Drake
 296 et al., 2006). Possible importance of the Fermi acceleration in magnetic flux ropes has
 297 been demonstrated also in recent 2D numerical simulations of magnetic reconnection (Arnold
 298 et al., 2021). Those simulations show that in case of not too large guide field, which is
 299 the case for the magnetotail reconnection, magnetic flux ropes can provide efficient ac-
 300 celeration of energetic electrons. Such a Fermi acceleration mechanism could work also
 301 in our case. First, the size of the cross-section of magnetic flux rope most probably is
 302 decreasing because flux rope should be gone once the jet pile-up region hits the near Earth
 303 dipolar field. Thus the decrease of the cross-section effectively leads to contraction of field
 304 lines with a following Fermi acceleration. Secondly, in 3D the flux rope should have a
 305 finite length in the direction along the core of the flux rope, corresponding to out-of-plane
 306 direction in 2D plots of a magnetic island. In such a case the initial build-up of the flux-
 307 rope’s core field efficiently corresponds to shortening the length of the field line between
 308 the ends of the flux rope. If there are trapped electrons inside the flux rope then this short-
 309 ening of the field lines will again effectively lead to Fermi acceleration. Thus, both mech-
 310 anisms separately or in combination can lead to Fermi acceleration inside the flux rope
 311 that we observe.

312 The few detailed case studies of electron acceleration inside flux ropes clearly show
 313 that more than one acceleration mechanism can be at play and more studies are needed
 314 to understand the relative importance of all those mechanisms. In addition, an impor-
 315 tant question remain of the relative importance of energetic electron acceleration mech-
 316 anisms due to acceleration inside the magnetic pile-up region and the turbulent region
 317 in front of the jet, including magnetic flux ropes. This requires further statistical stud-
 318 ies.

319 Finally, we discuss the second pile-up region that we mentioned discussing Figure 2
 320 and on which we zoom in Figure 7. The magnetic flux pile-up as seen in Figure 7a has
 321 very sharp and clear B_Z increase, there is a significant up to 500 km/s earthward V_X com-
 322 ponent, see Figure 7b, and as such this event has passed the criteria for earlier dipolar-
 323 ization front studies. However, in comparison to the first pile-up region, this event shows
 324 very low flux levels of high energy electrons, see Figure 7c,e. The thermal electron pop-
 325 ulation shown in Figure 7d shows that spacecraft are in the plasma sheet, with relatively
 326 small changes in the properties of the electron population. Also density observations in
 327 Figure 2e show that density varies inside the jet and the pile-up region but stays close
 328 to the surrounding values which is in contrast to the first pile-up region that shows very
 329 low densities. One possible explanation might be that the electrons in this second flux
 330 pile-up region were initially accelerated at a reconnection site different from the one as-
 331 sociated to the first pile-up region and associated to different plasma sheet source elec-
 332 trons. However, we find this unlikely since the two pile-up regions are observed with about
 333 10 minutes time differences during which the overall plasma sheet conditions around the
 334 reconnection site should have not changed substantially. Instead, our interpretation is
 335 that the second pile-up region is associated to a local flow enhancement which cant still
 336 be driven by a reconnection jet and jet braking, as for the first pile-up region, but it is
 337 not the reconnection jet itself. This interpretation is supported by the V_Y and $\mathbf{j} \times \mathbf{B}$ force
 338 observations, see Figure 7b,g. The V_Y is larger than the V_X and the $\mathbf{j} \times \mathbf{B}$ force in $-Y$
 339 direction, consistent with the pile-up region pushing the plasma in front of it in the $-Y$
 340 direction. This sideways motion can be generated by an incoming jet as it brakes or in-
 341 teracts with another reconnection jet ahead of it, and it pushes surrounding plasma side-
 342 ways. Such scenario was recently suggested by observations of two consecutive recon-
 343 nection jets, where the trailing jet had a V_Y much larger than V_X while for the leading
 344 jet the largest velocity was V_X (Catapano et al., 2021). Inside the second pile-up region
 345 there is some energetic electron energization in perpendicular direction, see Figure 7e,
 346 that is most probably caused by the betatron acceleration. However, following the arg-
 347 guments above, it is likely that such energetic electrons come from the pile-up of the lo-

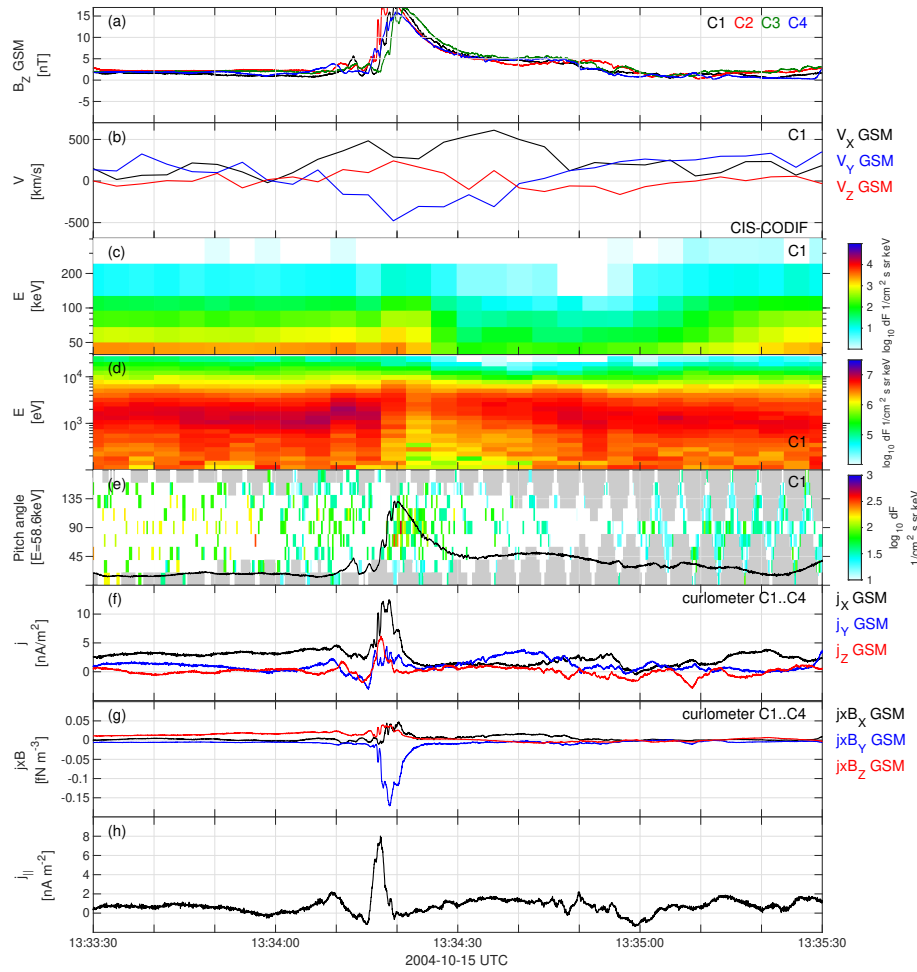


Figure 7. Second magnetic flux pile-up region. (a) B_Z in GSM, (b) plasma velocity in GSM, (c) high energy electron differential number flux, (d) electron differential number flux, (f) current in GSM based on curlometer method, (g) $\mathbf{j} \times \mathbf{B}$ -force in GSM, (h) current parallel to the ambient magnetic field.

348 cal plasma sheet plasma which has lower fluxes of energetic electrons compared to those
 349 with the reconnection jet itself. For this reason, the overall fluxes of energetic electrons
 350 stay small and this second pile-up region is less important for energetic electron genera-
 351 tion compared to the case where the piling-up plasma comes directly from the recon-
 352 nection site with preexisting high flux levels of energetic electrons, which is the case for
 353 the first pile-up region. The highest fluxes of energetic electrons in the magnetic flux pile-
 354 up and jet braking regions would then be expected for jets produced by lobe reconne-
 355 ction, as has been suggested also earlier in e.g. Vaivads et al. (2011). Although less im-
 356 portant for electron acceleration, the boundary in front of the second pile-up region shows
 357 strong parallel current, see Figure 7h, suggesting that this kind of pile-up regions can be
 358 important for field aligned coupling to the ionosphere.

4 Summary and conclusions

We present a detailed case study of energetic electron acceleration observed in the region where an earthward reconnection jet reaching up to 2000 km/s brakes close to the near-Earth dipolar-like field. We use data from Cluster spacecraft separated by ~ 1000 km that is comparable to the characteristic ion scales (gyroradius of thermal ions). Such separation is well suited for applying multi-spacecraft methods to estimate current and $\mathbf{j} \times \mathbf{B}$ force on characteristic ion kinetic scales in the region. We show that the energetic electrons are accelerated both in the magnetic flux pile-up region of the jet mainly through betatron acceleration, as well as in a turbulent region in front of the jet. Inside the turbulent region we can clearly identify a magnetic flux rope or magnetic island-like structure that shows the highest fluxes of energetic electron during the whole event. The highest acceleration region coincides with the center of the flux rope where we also observe the largest current during the event, including the largest field-aligned current. The energetic electrons inside the flux rope have the highest fluxes in the field-aligned directions consistent with being accelerated by either parallel electric field or Fermi acceleration due to contraction of the magnetic island. This event clearly demonstrates the importance of turbulent regions, including flux-rope-like structures, in front of reconnection jets in the acceleration of energetic electrons. In addition, we compare the event with the second magnetic flux pile-up region observed during the same interval but showing much lower fluxes of energetic electrons. The second pile-up region is most probably formed due to local flow enhancement in the plasma sheet and does not plasma coming directly from the reconnection site. We conclude that for highest electron energization it is important that the pile-up region is forming from plasma coming from the reconnection site with preexisting high levels of energetic electrons.

Acknowledgments

Cluster data are downloaded from Cluster Science Archive <https://csa.esac.esa.int/csa-web/>. We acknowledge the Cluster instrument CIS, EFW, FGM, PEACE, RAPID teams. AV acknowledges support from Swedish Research Council, grant 621-2013-4309. YK acknowledges support from the Swedish National Space Agency grant 139/18. EK is supported by German Research Foundation (DFG) under number KR 4375/2-1 within SPP "Dynamic Earth". PWD is supported by the Deutsches Zentrum für Luft- und Raumfahrt (DLR) under grant 50 OC 1602.

References

- Arnold, H., Drake, J. F., Swisdak, M., Guo, F., Dahlin, J. T., Chen, B., . . . Shen, C. (2021, March). Electron Acceleration during Macroscale Magnetic Reconnection. *Physical Review Letters*, *126*(13), 135101. doi: 10.1103/PhysRevLett.126.135101
- Åsnes, A., Friedel, R. W. H., Lavraud, B., Reeves, G. D., Taylor, M. G. G. T., & Daly, P. (2008). Statistical properties of tail plasma sheet electrons above 40 keV. *Journal of Geophysical Research: Space Physics*, *113*(A3). doi: 10.1029/2007JA012502
- Birn, J., Artemyev, A. V., Baker, D. N., Echim, M., Hoshino, M., & Zelenyi, L. M. (2012, November). Particle Acceleration in the Magnetotail and Aurora. *Space Science Reviews*, *173*(1), 49–102. doi: 10.1007/s11214-012-9874-4
- Borg, A. L., Taylor, M. G. G. T., & Eastwood, J. P. (2012, May). Observations of magnetic flux ropes during magnetic reconnection in the Earth's magnetotail. *Annales Geophysicae*, *30*(5), 761–773. doi: 10.5194/angeo-30-761-2012
- Catapano, F., Retinò, A., Zimbardo, G., Alexandrova, A., Cohen, I. J., Turner, D. L., . . . Burch, J. L. (2021, February). In Situ Evidence of Ion Acceleration between Consecutive Reconnection Jet Fronts. *The Astrophysical Journal*, *908*(1), 73. doi: 10.3847/1538-4357/abce5a

- 410 Chen, L.-J., Bhattacharjee, A., Puhl-Quinn, P. A., Yang, H., Bessho, N., Imada, S.,
 411 ... Georgescu, E. (2008, January). Observation of energetic electrons within
 412 magnetic islands. *Nature Physics*, *4*(1), 19–23. doi: 10.1038/nphys777
- 413 Drake, J. F., Swisdak, M., Che, H., & Shay, M. A. (2006, October). Electron ac-
 414 celeration from contracting magnetic islands during reconnection. *Nature*,
 415 *443*(7111), 553–556. doi: 10.1038/nature05116
- 416 Escoubet, C., Schmidt, R., & Goldstein, M. (1997, January). CLUSTER – SCI-
 417 ENCE AND MISSION OVERVIEW. *Space Science Reviews*, *79*(1), 11–32.
 418 doi: 10.1023/A:1004923124586
- 419 Fu, H. S., Cao, J. B., Khotyaintsev, Y. V., Sitnov, M. I., Runov, A., Fu, S. Y., ...
 420 Huang, S. Y. (2013). Dipolarization fronts as a consequence of transient re-
 421 connection: In situ evidence. *Geophysical Research Letters*, *40*(23), 6023–6027.
 422 doi: 10.1002/2013GL058620
- 423 Fu, H. S., Khotyaintsev, Y. V., André, M., & Vaivads, A. (2011, August). Fermi and
 424 betatron acceleration of suprathermal electrons behind dipolarization fronts.
 425 *Geophysical Research Letters*, *38*, L16104. doi: 10.1029/2011GL048528
- 426 Fu, H. S., Khotyaintsev, Y. V., Vaivads, A., André, M., Sergeev, V. A., Huang,
 427 S. Y., ... Daly, P. W. (2012, December). Pitch angle distribution of
 428 suprathermal electrons behind dipolarization fronts: A statistical overview.
 429 *Journal of Geophysical Research (Space Physics)*, *117*, A12221. doi:
 430 10.1029/2012JA018141
- 431 Hoshino, M., Mukai, T., Terasawa, T., & Shinohara, I. (2001). Suprathermal elec-
 432 tron acceleration in magnetic reconnection. *Journal of Geophysical Research:*
 433 *Space Physics*, *106*(A11), 25979–25997. doi: 10.1029/2001JA900052
- 434 Huang, S. Y., Vaivads, A., Khotyaintsev, Y. V., Zhou, M., Fu, H. S., Retinò, A.,
 435 ... Pang, Y. (2012). Electron acceleration in the reconnection diffusion
 436 region: Cluster observations. *Geophysical Research Letters*, *39*(11). doi:
 437 10.1029/2012GL051946
- 438 Imada, S., Nakamura, R., Daly, P. W., Hoshino, M., Baumjohann, W., Mühlbachler,
 439 S., ... Rème, H. (2007). Energetic electron acceleration in the downstream
 440 reconnection outflow region. *Journal of Geophysical Research: Space Physics*,
 441 *112*(A3). doi: 10.1029/2006JA011847
- 442 Khotyaintsev, Y. V., Cully, C. M., Vaivads, A., André, M., & Owen, C. J. (2011,
 443 April). Plasma Jet Braking: Energy Dissipation and Nonadiabatic Electrons.
 444 *Physical Review Letters*, *106*(16), 165001. doi: 10.1103/PhysRevLett.106
 445 .165001
- 446 Khotyaintsev, Y. V., Vaivads, A., André, M., Fujimoto, M., Retinò, A., & Owen,
 447 C. J. (2010, October). Observations of Slow Electron Holes at a Mag-
 448 netic Reconnection Site. *Physical Review Letters*, *105*, 165002. doi:
 449 10.1103/PhysRevLett.105.165002
- 450 Lapenta, G., Markidis, S., Goldman, M. V., & Newman, D. L. (2015, August).
 451 Secondary reconnection sites in reconnection-generated flux ropes and recon-
 452 nection fronts. *Nature Physics*, *11*(8), 690–695. doi: 10.1038/nphys3406
- 453 Lu, S., Artemyev, A. V., Angelopoulos, V., & Pritchett, P. L. (2020, June). Ener-
 454 getic Electron Acceleration by Ion-scale Magnetic Islands in Turbulent Mag-
 455 netic Reconnection: Particle-in-cell Simulations and ARTEMIS Observations.
 456 *The Astrophysical Journal*, *896*(2), 105. doi: 10.3847/1538-4357/ab908e
- 457 Luo, B., Tu, W., Li, X., Gong, J., Liu, S., des Rozières, E. B., & Baker, D. N. (2011).
 458 On energetic electrons (>38 keV) in the central plasma sheet: Data analysis
 459 and modeling. *Journal of Geophysical Research: Space Physics*, *116*(A9). doi:
 460 10.1029/2011JA016562
- 461 Malykhin, A. Y., Grigorenko, E. E., Kronberg, E. A., & Daly, P. W. (2018, Decem-
 462 ber). The Effect of the Betatron Mechanism on the Dynamics of Superthermal
 463 Electron Fluxes within Dipolarizations in the Magnetotail. *Geomagnetism and*
 464 *Aeronomy*, *58*(6), 744–752. doi: 10.1134/S0016793218060099

- 465 Malykhin, A. Y., Grigorenko, E. E., Kronberg, E. A., Koleva, R., Ganushkina,
 466 N. Y., Kozak, L., & Daly, P. W. (2018, May). Contrasting dynamics of
 467 electrons and protons in the near-Earth plasma sheet during dipolarization.
 468 *Annales Geophysicae*, *36*(3), 741–760. doi: 10.5194/angeo-36-741-2018
- 469 Oka, M., Fujimoto, M., Shinohara, I., & Phan, T. D. (2010). “Island surfing” mech-
 470 anism of electron acceleration during magnetic reconnection. *Journal of Geo-
 471 physical Research: Space Physics*, *115*(A8). doi: 10.1029/2010JA015392
- 472 Oka, M., Phan, T.-D., Krucker, S., Fujimoto, M., & Shinohara, I. (2010, April).
 473 ELECTRON ACCELERATION BY MULTI-ISLAND COALESCENCE. *The
 474 Astrophysical Journal*, *714*(1), 915–926. doi: 10.1088/0004-637X/714/1/915
- 475 Pritchett, P. L. (2006). Relativistic electron production during guide field magnetic
 476 reconnection. *Journal of Geophysical Research: Space Physics*, *111*(A10). doi:
 477 10.1029/2006JA011793
- 478 Retinò, A., Nakamura, R., Vaivads, A., Khotyaintsev, Y., Hayakawa, T., Tanaka,
 479 K., . . . Cornilleau-Wehrin, N. (2008). Cluster observations of energetic elec-
 480 trons and electromagnetic fields within a reconnecting thin current sheet in
 481 the Earth’s magnetotail. *Journal of Geophysical Research: Space Physics*,
 482 *113*(A12). doi: 10.1029/2008JA013511
- 483 Sitnov, M., Birn, J., Ferdousi, B., Gordeev, E., Khotyaintsev, Y., Merkin, V., . . .
 484 Zhou, X. (2019, June). Explosive Magnetotail Activity. *Space Science Reviews*,
 485 *215*(4). doi: 10.1007/s11214-019-0599-5
- 486 Vaivads, A., Retinò, A., Khotyaintsev, Y. V., & André, M. (2011, October).
 487 Suprathermal electron acceleration during reconnection onset in the magne-
 488 totail. *Annales Geophysicae*, *29*(10), 1917–1925. doi: 10.5194/angeo-29-1917-
 489 -2011
- 490 Zhong, Z. H., Zhou, M., Tang, R. X., Deng, X. H., Turner, D. L., Cohen, I. J., . . .
 491 Burch, J. L. (2020). Direct Evidence for Electron Acceleration Within Ion-
 492 Scale Flux Rope. *Geophysical Research Letters*, *47*(1), e2019GL085141. doi:
 493 10.1029/2019GL085141
- 494 Zhou, M., El-Alaoui, M., Lapenta, G., Berchem, J., Richard, R. L., Schriver, D., &
 495 Walker, R. J. (2018). Suprathermal Electron Acceleration in a Reconnecting
 496 Magnetotail: Large-Scale Kinetic Simulation. *Journal of Geophysical Research:
 497 Space Physics*, *123*(10), 8087–8108. doi: 10.1029/2018JA025502